Microchimica Acta (2022) 189: 91
https://doi.org/10.1007/s00604-022-05199-4

ORIGINAL PAPER

Portable electrochemical micro-workstation platform for simultaneous detection of multiple Alzheimer's disease biomarkers

Yibiao Liu[1] · Zhen Huang[1,2] · Qing Xu[3] · Lingyan Zhang[1] · Qiong Liu[3] · Tailin Xu[3]

Received: 16 December 2021 / Accepted: 24 January 2022 / Published online: 7 February 2022

Abstract

Alzheimer's disease, as a most prevalent type of dementia, is quickly becoming one of the most expensive, lethal, and burdening diseases of this century. Though there are still no efficient therapies, early diagnosis and intervention are important directive significance to clinical works. Here, we develop a portable electrochemical micro-workstation platform consisting of an electrochemical micro-workstation and integrated electrochemical microarray for simultaneously detecting multiple AD biomarkers including Aβ40, Aβ42, T-tau, and P-tau181 in serum. The integrated electrochemical microarray is mainly used for droplet sample manipulation and signal generation. The micro-workstation can regulate signals and transfer the signals to a smartphone by Bluetooth embedded inside. This portable electrochemical micro-workstation platform exhibits excellent analysis performance. The LODs for Aβ40, Aβ42, T-tau, and P-tau181 are 0.125 pg/mL, 0.089 pg/mL, 0.142 pg/mL, and 0.176 pg/mL, respectively, which satisfies the needs of detecting AD biomarkers in serum. The combination of portable micro-workstation and integrated electrochemical microarray provides a promising strategy for the early diagnosis of Alzheimer's disease and personal healthcare.

Keywords Electrochemical micro-workstation · Portable micro-workstation · High-throughput detection · AD biomarkers · Electrochemical biosensor · Microarray platform

Introduction

Alzheimer's disease is a most prevalent type of dementia, occurring mainly in aged people, and has become a critical threat to human life and health [1]. Although no reliable treatment for AD is available so far, a great deal of research demonstrated that early intervention in the early stage of AD is an important and effective strategy [1, 2]. Therefore, early diagnosis is essential for clinical treatment. The positron-emission tomography (PET) and the level of β-amyloid peptide (Aβ40, Aβ42), T-tau, and P-tau181 in cerebrospinal fluid (CSF) are gold standard of AD clinical diagnosis [1, 3]. However, the detection based on PET and CSF biomarkers is difficult to use for general screening in the public because of high cost, invasivity, and unavailability. Therefore, establishing portable, low-cost, and noninvasive quantitative detective methods of AD blood markers, such as Aβ40, Aβ42, T-tau, and P-tau181, is required [4, 5]. In the blood, the physiological concentration of AD blood markers is level of approximate picograms per milliliter, which is out of measurement limit of a classic method, enzyme-linked immunosorbent assay (ELISA). To date, a great deal of analytical method has been developed to detect AD blood biomarkers (Aβ40, Aβ42, T-tau, and P-tau181), including ion mobility-mass spectrometry (IM-MS) [6], colorimetric [7], electrochemical [8–10], fluorescence [11, 12], and surface-enhanced Raman spectroscopy (SERS) [13]. Among them, electrochemical biosensors exhibited great potential for disease diagnosis and personal healthcare because of high sensitivity, rapid response, low cost, and easy miniaturization.

Yibiao Liu, Zhen Huang, and Qing Xu are co-first authors

✉ Qiong Liu
liuqiong@szu.edu.cn

✉ Tailin Xu
xutailin@szu.edu.cn

[1] Longgang District Central Hospital of Shenzhen, Shenzhen, China

[2] Office of Shenzhen Clinical College, Guangzhou University of Chinese Medicine, Longggang District Central Hospital, Shenzhen, China

[3] School of Biomedical Engineering, Health Science Center, College of Life Sciences and Oceanography, Shenzhen University, Shenzhen 518060, Guangdong, China

Microarray-based sensing technologies have been widely used in drug discovery, biosensors, and high-throughput analysis [14–18]. The traditional array sensing technologies use 96-, 384-, or more well plates as a carrier. The samples are restricted in microcavities so that solution manipulation and signal collection is limited [19, 20]. By contrast, open-channel droplet-based sensing platforms is used for biosensing due to easy droplet control, low sample consumption, and multiple signal acquisition [21–28] Recently, open-channel droplet sensing platforms based on mini-pillar have achieved 3D cell cultures and high-throughput analysis [29, 30], which was easy to form stable droplet arrays regardless of the extremely physical and chemical properties. Most mini-pillar sensing platforms acquire signals in droplets by colorimetry or fluorescence [29]. Recently, our group reported an integrated electrochemical microarray sensor based on mini-pillar for detecting biomarker of disease [9, 19]. Each electrochemical unit is separated by mini-pillar, which reduces the interferences compared to the typical electrode arrays that all the electrodes were in the same sample solution [31, 32]. Although these electrochemical microarray sensor platforms exhibited excellent performance, they also need electrochemical workstation in laboratory so that they cannot be difficult to use for point of care test or personal healthcare at home.

In this work, we developed a portable electrochemical micro-workstation platform consisting of an electrochemical micro-workstation (size: 2 cm × 1 cm × 0.5 cm) and mini-pillar-based electrochemical microarray (size: 4 cm × 4 cm) for simultaneously detecting multiple AD biomarkers in blood (Fig. 1a). The electrochemical microarray based on mini-pillar is used for droplet sample manipulation and signal generation. The micro-workstation is applied to signal regulation and collection. Moreover, the signals are also transferred to a smartphone by Bluetooth embedded inside. As shown in Fig. 1, this electrochemical microarray integrates 4 × 4 mini-pillar array (J1 to J16)–embedded three-electrode and a circuit for high-throughput analysis. On the surface of mini-pillar, each electrochemical unit can acquire electrochemical signals in droplets, and all the electrochemical units based on a three-electrode system are integrated together and form a high-throughput electrochemical microarray platform. Each electrochemical unit based on mini-pillar is individual, which eliminates signal interference and cross-contamination. In this portable sensing platform, the micro-workstation is used for signal regulation and collection, and then, the signals are transferred to a smartphone by Bluetooth embedded inside. Figure 1b shows the circuit of the electrochemical microarray and internal structure of micro-workstation. As can be seen in Fig. 1c, the micro-workstation consists of a microcontroller (1), resistance–capacitance (2), linear

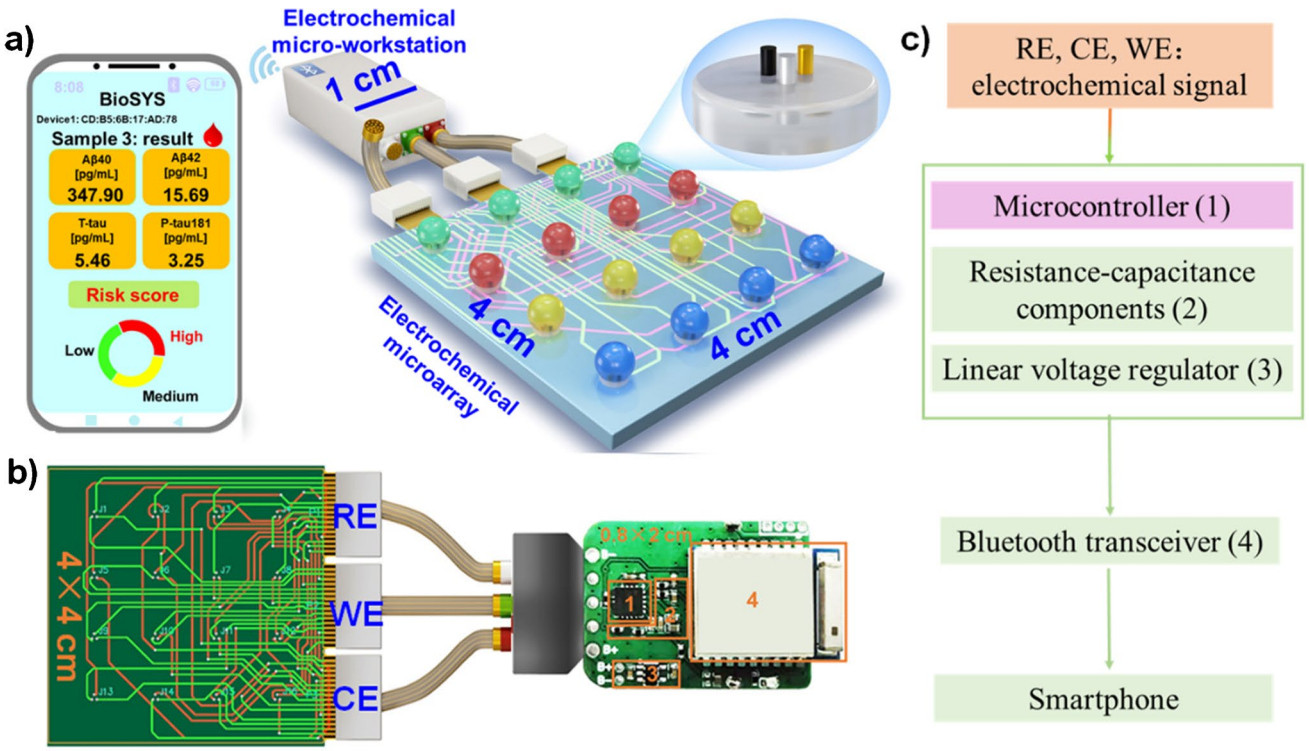

Fig. 1 **a** The schematic illustration of portable electrochemical micro-workstation platform. **b** A real picture of this electrochemical microarray. **c** Internal structure of micro-workstation. RE, CE, and WE represent reference electrode, counter electrode, and working electrode, respectively

voltage regulator (3), and Bluetooth transceiver (4). Based on this portable electrochemical micro-workstation platform, we successfully accomplished highly sensitive multiple AD biomarker (Aβ40, Aβ42, T-tau, P-tau181) detection in serum. This portable electrochemical micro-workstation platform exhibits excellent analysis performance, providing a promising strategy for the early diagnosis of Alzheimer's disease and personal healthcare.

Experiment section

Apparatus and reagents

Aβ peptides (Aβ40 and Aβ42), T-tau, P-tau181, and their antibody were obtained from Abcam (Hong Kong) Ltd., and were stored at – 20 °C. DNA aptamer of T-tau (5′-SH-(CH2)6-CAG CACCGTCAACTGAATGGGTTGGCCGGGCAGCGGGGG GTAGGC TTGGTGATGCGATGGAGATGT-3′) screened by Tan et al. [33] was synthesized by Sangon Biotech Co., Ltd. (Shanghai, China), and was stored at 4 °C. The antibody and protein, and DNA bovine serum albumin (BSA), ferrocene, sodium chloride (NaCl), potassium chloride (KCl), $Na_2HPO_4 \bullet 12H_2O$, potassium ferricyanide/ferrocyanide, and KH_2PO4 were purchased from Sigma-Aldrich. The polydimethylsiloxane (PDMS, Sylgard 184) was purchased from Dow Corning. All chemicals were of analytical grade. Ultrapure water (Milli-Q, 18.2 MΩ cm) was used in all experiments.

Characterization and measurement

The electrode surface morphology was characterized using field emission scanning electron microscopy (SEM, FEI Apreo S, USA). All the electrochemical measurements were performed by portable electrochemical micro-workstation. The electrochemical micro-workstation was customized from Refresh AI Biosensor Co., Ltd. according to our design.

Fabrication of electrochemical microarray

The electrochemical microarray consists of mini-pillar platform, and an electrochemical circuit consists of many sensing units. The electrochemical microarray was fabricated according to ref. [19]. Briefly, PDMS and curing agent with a ratio of 16:1 were mixed and stirred. Then, the bubbles were pumped out by means of vacuum-drying oven. Next, the PDMS prepolymer was dumped on the polytetrafluoroethylene (PTEE) template (4 × 4), and the three electrodes (Au as working electrode, Pt wire as counter electrode, and Ag/AgCl as reference electrode) were embedded in the prepolymer. After 6 h solidification at 60 °C and stripping the template, the PDMS mini-pillar with electrode arrays was obtained.

Preparation of electrochemical biosensor based on microarray

The construction of electrochemical biosensor based on microarray was performed according to the following steps. Firstly, all the Au electrode surface was modified with nano-Au by electrodeposition in 10 mM $HAuCl_4$. The deposition voltage is – 1.4 V, and deposition time is 300 s. Then, the antibody (Aβ40, Aβ42, P-tau181) and DNA aptamer of T-tau (10 μM) were dropped onto the surface and incubated for 1 h at 37 °C. Then, bovine serum albumin (BSA, 1%) was used to block the nonspecific binding sites. Finally, 10 μL antigen solution was added to the mini-pillar surface (1 h at 37 °C). After each step, the mini-pillar surface was washed three times with phosphate-buffered solution (PBS) (0.01 M, pH = 7.4). The measurement of antigen was performed by a portable electrochemical micro-workstation. The electrochemical assay was carried out by chronoamperometry (the working potential was – 0.05 V) and differential pulse voltammetry (DPV, the working potential ranges from 0 to 0.4 V). After incubation with different concentrations of the antigen, the variations of current (ΔI) were recorded correspondingly and were used for quantifying antigen (Aβ40, Aβ42, P-tau181, T-tau) level. The selectivity of sensor was investigated in PBS buffer containing BSA, Aβ40, Aβ42, Tau441, and P-tau181.

Human serum sample test

The performance of this portable electrochemical microworkstation platform in human serum was carried out by chronoamperometry and DPV. (Human serum was obtained from Shenzhen University General Hospital.) Simply, 10 μL sample (2 μL serum diluted with 8 μL PBS buffer) was added to each mini-pillar surface and incubated for 1 h at 37 °C. The portable sensing system was placed in a constant humidity box against droplet evaporation. At last, the ΔI signals were recorded.

Results and discussions

Fabrication and characterization of portable electrochemical micro-workstation platform based on mini-pillar

The electrochemical microarray was fabricated according to our previous report [19]. The procedures of integrating circuit unit and PDMS mini-pillar are shown in Fig. 2a. Firstly, the mini-pillar and circuit board were glued, and then, the three electrodes (Pt wires as counter electrode, Au wires as working electrode, and Ag/AgCl as reference electrode) were embedded in the mini-pillar, and the

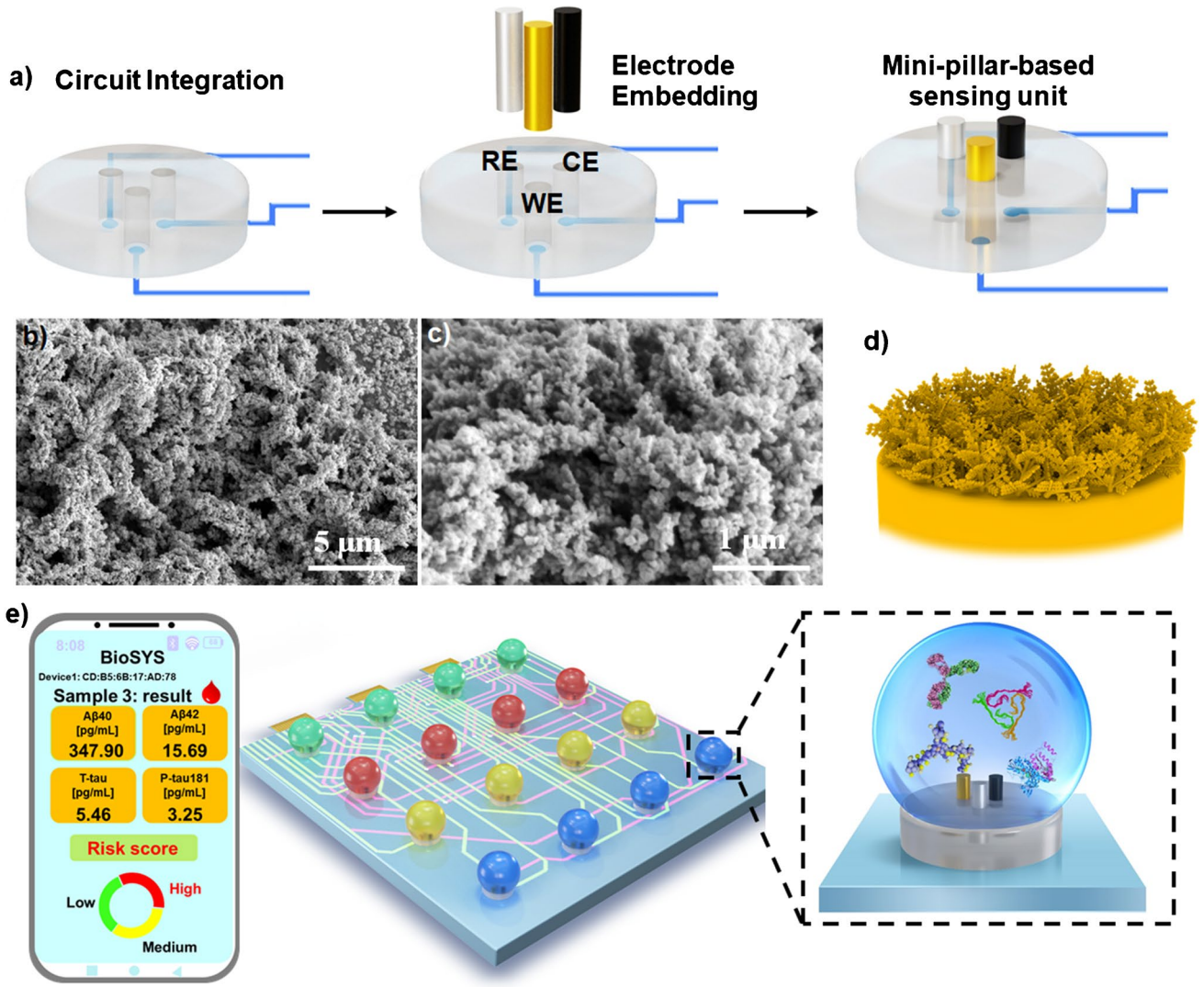

Fig. 2 Design and construction of the mini-pillar-based portable electrochemical sensing. **a** Assembly of the electrodes in the PDMS mini-pillar. **b-d** the morphology characterization of nano-Au structures on the surface of working electrodes. **e** The schematic illustration of portable electrochemical sensing platform for detecting AD biomarkers

bottom of electrode wires was welded with the integrated circuit board. By now, an electrochemical microarray based on mini-pillar was prepared. To further improve the sensitivity of this electrochemical microarray, the Au wire electrode surface was modified with nano-Au by electrodeposition. The deposition voltage is – 1.4 V, and deposition time is 300 s. Then, the morphology of obtained nano-Au was characterized as shown in Fig. 2b-d, and a nano-dendritic structure was observed. This nano-dendritic Au structure can decrease the limit of detection and improve the sensitivity of sensor due to higher density and larger electroactive area. Afterwards, antibody or DNA aptamer was modified on the surface of nano-Au.

To explore the ability of anchoring droplet, PDMS and curing agent with different ratios (8:1, 10:1, 12:1, 14:1, 16:1, 18:1) was prepared for mini-pillar array. The adhesion force was measured as shown in Fig. S1, and the results demonstrated that the maximum adhesion forces gradually enhanced with the increasing ratio of PDMS and curing agent. When the ratio exceeds 16:1, the maximum adhesion forces have little changed. Therefore, we select the ratio of 16:1 for preparing the PDMS mini-pillar. Moreover, PDMS mini-pillar also displayed outstanding ability against complex samples such as juice, coffee, milk, and serum (Fig. S2a). In addition, the PDMS mini-pillar exhibits an excellent anchor droplet ability regardless of rotation of 90°, even 180° (Fig. S2b, c). In order to apply aforementioned

electrochemical microarray directly to POCT or personal healthcare, a portable electrochemical micro-workstation capable of connecting to a smartphone via Bluetooth was customized. The detection result could be shown in a smartphone app (Fig. 2e). Finally, the portable electrochemical micro-workstation platform for detecting AD biomarkers was constructed by the combination of the micro-workstation and electrochemical microarray.

Analytical performance of portable electrochemical micro-workstation platform

The analytical performances of the portable electrochemical micro-workstation platform were systematically characterized as shown in Fig. 3. Firstly, the electroactive area of working electrodes was evaluated by cyclic voltammetry (CV), and the result showed electroactive area of nano-Au is much larger than that of Au wires (Fig. 3a). Moreover, the CV was carried out at different scan rates varied from 50, 100, 150, 200, to 400 mV/s in 10 μL PBS (10 mM, pH 7.4) containing 0.1 M KCl and 10 mM potassium ferricyanide/ferrocyanide. As can be seen in Fig. 3b, a linear relationship between the peak current and scan rate with a correlation coefficient of 0.993 was observed, and the oxidation and the reduction peak currents were nearly symmetric, which indicated that the redox process on the mini-pillar surface was a diffusion-limited process. To investigate the uniformity of each electrochemical unit, CVs under the same conditions were performed by electrochemical micro-workstation. The results show that the peak currents of each electrochemical unit (J1 to J16) have no significant differences, indicating an excellent uniformity of this portable electrochemical micro-workstation platform (Fig. 3c and Fig. S3).

To obtain better sensing performance in the detection of target protein (Aβ40, Aβ42, T-tau, P-tau181), the concentration of antibody (Aβ40, Aβ42, P-tau181) or DNA aptamer (T-tau) was optimized. As shown in Fig. S4, an optimal antibody concentration was 50 ng/mL, and an optimal DNA aptamer concentration was 10 μM.

Under the optimal conditions, the as-fabricated portable electrochemical micro-workstation platform was applied to quantitatively simultaneous detect four AD biomarkers including Aβ40, Aβ42, T-tau, and P-tau181 by DPV and chronoamperometry. For Aβ40, Aβ42, and P-tau181, the corresponding antibody was modified on the nano-Au surface, and then, the BSA was used to block the nonspecific adsorption sites. Next, the different concentration of antigen (Aβ40, Aβ42, P-tau181) was dropped on the electrode surface and incubated for 1 h at 37 °C. Finally, the HRP-labeled antibody was added to the corresponding electrode surface. These AD biomarkers including Aβ40, Aβ42, and P-tau181 are detected by chronoamperometry. As shown in Fig. 3d, horse reddish peroxidase (HRP) catalyzes the breakdown of H_2O_2. When the potential is − 0.05 V, the instantaneous current change reaches the maximum. The concentration of target proteins is measured by instantaneous current change (ΔI) at − 0.05 V before and after adding H_2O_2. The detection of T-tau is based on the resistance change of nano-Au electrode surface as shown in Fig. 3e. The DNA aptamer specifically recognizes T-tau resulting in a conformational change, which increases the surface resistance causing signal reduction. The concentration of T-tau was measured according to the peak current change at 0.21 V before and after adding T-tau.

The electrochemical signals of multiple AD biomarkers including Aβ40, Aβ42, T-tau, and P-tau181 were recorded by electrochemical micro-workstation platform. As can be seen in Fig. 3f and g, the current variation (ΔI) enhanced as the target antigen concentration increased. The ΔI and logarithm of target antigen concentration exhibited a good linear relationship from 0.1 to 1000 pg/mL. The detection limit of this electrochemical micro-workstation platform for Aβ40 is about 0.142 pg/mL ($S/N = 3$). The sensitivity of this sensor for Aβ40 is 134 (μA/pg mL^{-1})/cm^2. (slope/electrode area) [34]. The limit of detection (LOD) is calculated by three times the standard deviation of the blank [10, 35, 36]. The response of the blank is shown in Fig. S5. Similarly, the LOD of T-tau, Aβ42, and P-tau181 is 0.089 pg/mL, 0.125 pg/mL, and 0.176 pg/mL, respectively. The sensitivity for T-tau, Aβ42, and P-tau181 is 560.3 (μA/pg mL^{-1})/cm^2, 91.72 (μA/pg mL^{-1})/cm^2, and 86.6 (μA/pg mL^{-1})/cm^2, respectively. Moreover, the limit of quantification (LOQ) is also calculated by measuring the signal of the blank plus ten times standard deviation of blank. The LOQ of this sensor for Aβ40 is 0.199 pg/mL. Similarly, the LOQ of T-tau, Aβ42, and P-tau181 is 0.212 pg/mL, 0.182 pg/mL, and 0.293 pg/mL, respectively. In blood, the physiological concentration of Aβ40, Aβ42, T-tau, and P-tau181 was about several to hundreds of picograms per milliliter. This result demonstrated that our developed electrochemical micro-workstation platform satisfied the needs of detecting AD biomarkers in blood. As a comparison, a classical method, ELISA, was used to verify the electrochemical micro-workstation platform. The ELISA calibration curve was constructed by plotting the optical density of antigen (Aβ40, Aβ42, T-tau, P-tau181) at 450 nm (TMB as substrate). As can be seen in Fig. S6, the linear range of sensing unit for Aβ40 is 10–1000 pg/mL. Similarly, the linear range for Aβ42, T-tau, and P-tau181 is 10–800 pg/mL, 10–500 pg/mL, and 10–500 pg/mL, respectively. The LOD was calculated, and the LOD of this sensing unit for Aβ40, Aβ42, T-tau, and P-tau181 was 18.6 pg/mL, 9.6 pg/mL, 8.9 pg/mL, and 16.88 pg/mL, respectively. Compared with typical

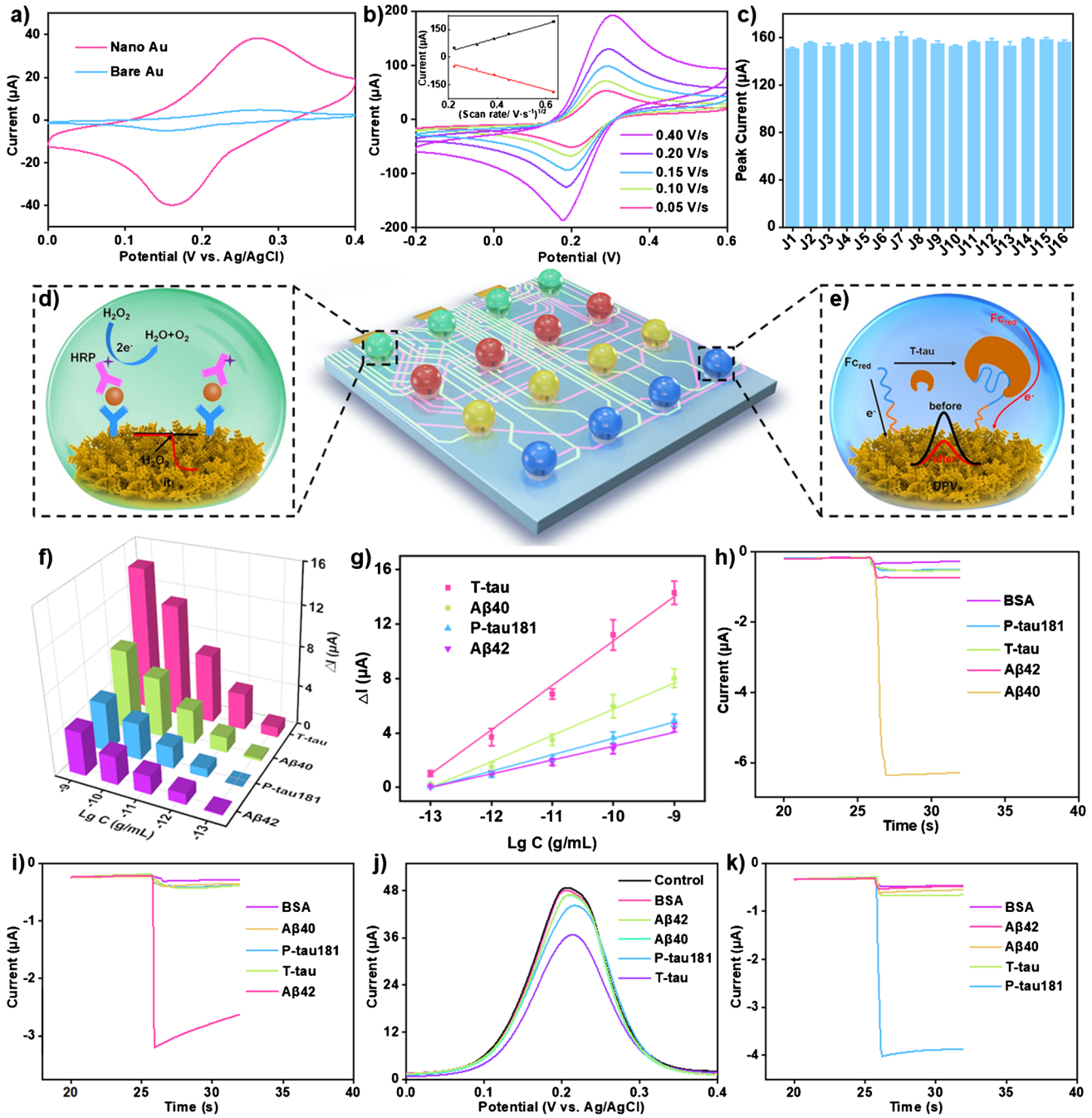

Fig. 3 The analytical performance of the portable electrochemical sensing platform for the detection of AD biomarkers. **a** CVs of bare Au and nano-Au in 5 mM $K_3[Fe(CN)_6]/K_4[Fe(CN)_6]$ solution containing 0.1 M KCl at 100 $mV{\cdot}s^{-1}$. **b** CVs of each electrochemical sensing unit at different scan rates ranging from 0.05 to 0.40 V/s. **c** the peak currents of CVs measured by each electrochemical sensing unit (J1 to J16) **d** The mechanism of electrochemical detection of Aβ40, Aβ42, and P-tau181. (The working potential is − 0.05 V). **e** The detection mechanism of T-tau (The peak potential is 0.21 V). **f** Electrochemical signals of different concentration biomarkers (magenta: T-tau; green: Aβ40; blue: P-tau181; purple: Aβ42;). **g** The corresponding calibration curve. h–k The selectivity of this portable electrochemical sensing platform

ELISA, our developed electrochemical micro-workstation platform based on mini-pillar exhibited lower LOD and wider linear range. A comparison between our method and previous reports' method is shown in Table 1.

Selectivity and stability

In biological application, the stability and specificity are very crucial factors for the construction of biosensor. The

Table 1 Comparison of developed electrochemical micro-workstation platform with other methods for detecting AD biomarkers

Methods	Target	LOD	Reference
Fluorescence	Aβ42, tau441, p-tau181,	340.07, 669.44, 493.79 pg/mL	[37]
Electrochemical	Tau, p-tau181, Aβ42, Aβ40	2.45, 2.72, 2.13, 2.20 fM	[38]
SERS	Tau, Aβ42 oligomers	4.2×10^{-4} pM 3.7×10^{-2} nM	[39]
Electrochemical	miRNA-101, ApoE4, Tau, Aβ	91.4 pM; 5.91×10^{-11}; 7.14×10^{-11}; 8.6×10^{-12} mg/mL	[9]
LSPR	Aβ40, Aβ42, T-tau	34.9 fM, 26 fM, 23.6 fM	[40]
Electrochemical	Aβ42	0.146 fg/mL	[34]
Multiplex biosensor	Aβ, tau	0.2 fM, 2.2 fM	[41]
FET sensors	Tau	10 fg/mL	[42]
Electrochemical	Aβ	1 pg/mL	[43]
Electrochemical	T-tau, p-tau181, Aβ40, Aβ42	0.125, 0.089, 0.142, 0.176 pg/mL	This work

selectivity and stability of our developed portable electrochemical micro-workstation platform was assessed. As shown in Fig. 3h, when the 100 pg/mL Aβ40 existed on sensing unit detecting Aβ40, an obvious signal response of 6.21 mm^2 was observed. On this sensing unit surface, while the concentration of other protein is 100-fold higher than that of Aβ40, the ΔI for BSA, P-tau181, Aβ42, and T-tau was 0.18, 0.35, 0.60, and 0.43 μA, which accounted for 2.89%, 5.63%, 9.66%, and 6.92% of the ΔI for Aβ40, respectively. Similarly, for Aβ42 sensing unit, the signal response is about 2.78 μA. ΔI for BSA, P-tau181, Aβ40, and T-tau was 0.08, 0.16, 0.26, and 0.22 μA, which accounted for 2.87%, 5.75%, 9.35%, and 7.91% of the ΔI for Aβ42, respectively (Fig. 3i). Likewise, for T-tau or P-tau181, the corresponding sensing unit both exhibited excellent selectivity (Fig. 3j and k). These results showed that the selectivity of this electrochemical micro-workstation platform was acceptable. Moreover, the stability of portable electrochemical micro-workstation platform was evaluated by conducting multiple trials of 100 pg/mL antigen (Aβ40, Aβ42, T-tau, P-tau181) detection (Fig. S7). The result proves that this electrochemical sensing platform has excellent stability.

The application of electrochemical platform in human serum

To further evaluate the clinical potential of the portable electrochemical micro-workstation platform, Aβ40, Aβ42, T-tau, and P-tau181 of three human serum samples were detected by our designed sensing platform and typical ELISA. The results are shown in Table 2. In human serum samples, Aβ40 and Aβ42 can be both detected by typical ELISA and our sensing platform, and they had negligible difference. This result indicated that our developed portable sensing platform could be used for detecting the clinical samples. Moreover, T-tau and P-tau181 were detected by our method, but was not detected by typical ELISA, which demonstrated that this portable sensing platform has lower LOD than typical ELISA. These results proved that this portable electrochemical sensing platform can be applied to the detection of multiple AD biomarkers in biological sample. To sum up, the portable sensing platform exhibits excellent analytical performance; there are some limitations such as long incubation time. In a follow-up study, we try to improve the reaction speed by ultrasonic agitation, decreasing the incubation time.

Table 2 Comparison between our portable electrochemical micro-workstation platform and typical ELISA for AD biomarkers in human serum sample

Sample	Biomarkers	Average measured concentration (pg/mL)	
		This electrochemical sensing platform	ELISA
1	Aβ40	167.75 ± 10.63	172.50 ± 8.68
	Aβ42	12.42 ± 1.03	12.12 ± 0.96
	T-tau	2.59 ± 0.15	/
	P-tau181	2.32 ± 0.12	/
2	Aβ40	224.58 ± 12.48	222.65 ± 8.33
	Aβ42	20.88 ± 1.12	21.26 ± 0.88
	T-tau	3.89 ± 0.16	/
	P-tau181	2.03 ± 0.15	/
3	Aβ40	347.90 ± 15.36	360.32 ± 8.62
	Aβ42	15.69 ± 1.16	16.08 ± 0.82
	T-tau	5.46 ± 0.14	/
	P-tau181	3.25 ± 0.12	/

Conclusions

In conclusion, we combined an electrochemical micro-workstation with integrated electrochemical microarray and developed a portable, high-throughput electrochemical

micro-workstation platform for simultaneously detecting multiple AD biomarkers in serum. This portable electrochemical micro-workstation platform displayed outstanding analytical performance with a lower detection limit and a wide linear range. The LOD of each sensing unit for Aβ40, Aβ42, T-tau, and P-tau181 was 0.142 pg/mL, 0.125 pg/mL, 0.089 pg/mL, and 0.176 pg/mL, respectively. This result satisfies the need of detecting AD biomarkers in serum. In addition, the portable electrochemical micro-workstation was not only used for signal regulation, but also for transferring signals to the smartphone by Bluetooth embedded inside. The portable electrochemical micro-workstation platform provides a promising strategy for the early diagnosis of Alzheimer's disease and personal healthcare.

Supplementary Information The online version contains supplementary material available at https://doi.org/10.1007/s00604-022-05199-4.

Acknowledgements We thank the Instrumental Analysis Center of Shenzhen University (Xili Campus) for providing access to the instruments used in the experiments.

Funding The work was supported by Longgang District Medical and health science and technology project (LGKCYLWS2021000003), the National Natural Science Foundation of China (21804007, 21890742), SZU Top Ranking Project (86000000210), Shenzhen Key Laboratory for Nano-Biosensing Technology (ZDSYS20210112161400001), and Shenzhen Stability Support Plan (20200806163622001).

Declarations

Conflict of interest The authors declare no competing interests.

References

1. Li Y, Haber A, Preuss C, John C, Uyar A, Yang HS, Logsdon BA, Philip V, Karuturi RKM, Carter GW, Initia ADN (2021) Transfer learning-trained convolutional neural networks identify novel MRI biomarkers of Alzheimer's disease progression. Alzheimer's & Dementia: Diagnosis, Assessment & Disease Monitoring 13(1):1–14. https://doi.org/10.1002/dad2.12140
2. Scheltens P, Blennow K, Breteler MMB, de Strooper B, Frisoni GB, Salloway S, Van der Flier WM (2016) Alzheimer's disease. The Lancet 388(10043):505–517. https://doi.org/10.1016/s0140-6736(15)01124-1
3. Marcus C, Mena E, Subramaniam RM (2014) Brain PET in the diagnosis of Alzheimer's disease. Clin Nucl Med 39 (10):e413–422; quiz e423–416. https://doi.org/10.1097/RLU.0000000000000547
4. Nakamura A, Kaneko N, Villemagne VL, Kato T, Doecke J, Dore V, Fowler C, Li QX, Martins R, Rowe C, Tomita T, Matsuzaki K, Ishii K, Ishii K, Arahata Y, Iwamoto S, Ito K, Tanaka K, Masters CL, Yanagisawa K (2018) High performance plasma amyloid-beta biomarkers for Alzheimer's disease. Nature 554(7691):249–254. https://doi.org/10.1038/nature25456
5. Brazaca LC, Sampaio I, Zucolotto V, Janegitz BC (2020) Applications of biosensors in Alzheimer's disease diagnosis. Talanta 210:120644. https://doi.org/10.1016/j.talanta.2019.120644
6. Obata Y, Murakami K, Kawase T, Hirose K, Izuo N, Shimizu T, Irie K (2020) Detection of amyloid β oligomers with RNA aptamers in AppNL-G-F/NL-G-F mice: a model of arctic Alzheimer's disease. ACS Omega 5(34):21531–21537. https://doi.org/10.1021/acsomega.0c02134
7. Zhou X, Wang S, Zhang C, Lin Y, Lv J, Hu S, Zhang S, Li M (2021) Colorimetric determination of amyloid-beta peptide using MOF-derived nanozyme based on porous ZnO-Co3O4 nanocages. Mikrochim Acta 188(2):56. https://doi.org/10.1007/s00604-021-04705-4
8. Wang Y, Fan D, Zhao G, Feng J, Wei D, Zhang N, Cao W, Du B, Wei Q (2018) Ultrasensitive photoelectrochemical immunosensor for the detection of amyloid beta-protein based on SnO2/SnS2/Ag2S nanocomposites. Biosens Bioelectron 120:1–7. https://doi.org/10.1016/j.bios.2018.08.026
9. Song Y, Xu T, Zhu Q, Zhang X (2020) Integrated individually electrochemical array for simultaneously detecting multiple Alzheimer's biomarkers. Biosens Bioelectron 162:112253. https://doi.org/10.1016/j.bios.2020.112253
10. Liu Y, Xu Q, Zhang Y, Ren B, Huang L, Cai H, Xu T, Liu Q, Zhang X (2021) An electrochemical aptasensor based on AuPt alloy nanoparticles for ultrasensitive detection of amyloid-beta oligomers. Talanta 231:122360. https://doi.org/10.1016/j.talanta.2021.122360
11. Wang XZ, Du J, Xiao NN, Zhang Y, Fei L, LaCoste JD, Huang Z, Wang Q, Wang XR, Ding B (2020) Driving force to detect Alzheimer's disease biomarkers: application of a thioflavine T@Er-MOF ratiometric fluorescent sensor for smart detection of presenilin 1, amyloid beta-protein and acetylcholine. Analyst 145(13):4646–4663. https://doi.org/10.1039/d0an00440e
12. Fang WK, Liu L, Zhang LL, Liu D, Liu Y, Tang HW (2021) Detection of amyloid beta oligomers by a fluorescence ratio strategy based on optically trapped highly doped upconversion nanoparticles-SiO2@metal-organic framework microspheres. Anal Chem 93(36):12447–12455. https://doi.org/10.1021/acs.analchem.1c02679
13. Yang JK, Hwang IJ, Cha MG, Kim HI, Yim D, Jeong DH, Lee YS, Kim JH (2019) Reaction kinetics-mediated control over silver nanogap shells as surface-enhanced Raman scattering nanoprobes for detection of Alzheimer's disease biomarkers. Small 15(19):e1900613. https://doi.org/10.1002/smll.201900613
14. Miranda OR, Chen HT, You CC, Mortenson DE, Yang XC, Bunz UH, Rotello VM (2010) Enzyme-amplified array sensing of proteins in solution and in biofluids. J Am Chem Soc 132(14):5285–5289. https://doi.org/10.1021/ja1006756
15. Chi J, Shao C, Du X, Liu H, Gu Z (2018) Generating microdroplet array on photonic pseudo-paper for absolute quantification of nucleic acids. ACS Appl Mater Interfaces 10(45):39144–39150. https://doi.org/10.1021/acsami.8b11552
16. Nie B, Li R, Brandt JD, Pan T (2014) Iontronic microdroplet array for flexible ultrasensitive tactile sensing. Lab Chip 14(6):1107–1116. https://doi.org/10.1039/c3lc50994j
17. Welch CJ (2019) High throughput analysis enables high throughput experimentation in pharmaceutical process research. Reaction Chemistry & Engineering 4(11):1895–1911. https://doi.org/10.1039/c9re00234k
18. Xu T, Song Y, Gao W, Wu T, Xu LP, Zhang X, Wang S (2018) Superwettable electrochemical biosensor toward detection of cancer biomarkers. ACS Sens 3(1):72–78. https://doi.org/10.1021/acssensors.7b00868
19. Song YC, Xu TL, Song X, Zhang XJ (2020) Integrated microdroplets array for intelligent electrochemical fabrication. Advanced Functional Materials 30 (13). https://doi.org/10.1002/adfm.201910329
20. Mark D, Haeberle S, Roth G, von Stetten F, Zengerle R (2010) Microfluidic lab-on-a-chip platforms: requirements, characteristics and applications. Chem Soc Rev 39(3):1153–1182. https://doi.org/10.1039/b820557b

21. Kunding AH, Busk LL, Webb H, Klafki HW, Otto M, Kutter JP, Dufva M (2018) Micro-droplet arrays for micro-compartmentalization using an air/water interface. Lab Chip 18(18):2797–2805. https://doi.org/10.1039/c8lc00608c
22. Mao P, Cao L, Li Z, You M, Gao B, Xie X, Xue Z, Peng P, Yao C, Xu F (2021) A digitalized isothermal nucleic acid testing platform based on a pump-free open droplet array microfluidic chip. Analyst 146(22):6960–6969. https://doi.org/10.1039/d1an01373d
23. Brutin D, Starov V (2018) Recent advances in droplet wetting and evaporation. Chem Soc Rev 47(2):558–585. https://doi.org/10.1039/c6cs00902f
24. Dong R, Zhang T, Feng X (2018) Interface-assisted synthesis of 2D materials: trend and challenges. Chem Rev 118(13):6189–6235. https://doi.org/10.1021/acs.chemrev.8b00056
25. Feng W, Ueda E, Levkin PA (2018) Droplet microarrays: from surface patterning to high-throughput applications. Adv Mater 30(20):e1706111. https://doi.org/10.1002/adma.201706111
26. He X, Xu T, Gao W, Xu LP, Pan T, Zhang X (2018) Flexible superwettable tapes for on-site detection of heavy metals. Anal Chem 90(24):14105–14110. https://doi.org/10.1021/acs.analchem.8b04536
27. Zhan SS, Pan Y, Gao ZF, Lou XD, Xia F (2018) Biological and chemical sensing applications based on special wettable surfaces. Trac-Trends in Analytical Chemistry 108:183–194. https://doi.org/10.1016/j.trac.2018.09.001
28. Li ZH, Song YC, Fan C, Xu TL, Zhang XJ (2021) Mini-pillar based multi-channel electrochemical platform for studying the multifactor silver electrodeposition. Electroanalysis 33(12):2401–2405. https://doi.org/10.1002/elan.202100462
29. Kang J, Lee DW, Hwang HJ, Yeon SE, Lee MY, Kuh HJ (2016) Mini-pillar array for hydrogel-supported 3D culture and high-content histologic analysis of human tumor spheroids. Lab Chip 16(12):2265–2276. https://doi.org/10.1039/c6lc00526h
30. Li J, Tan W, Xiao W, Carney RP, Men Y, Li Y, Quon G, Ajena Y, Lam KS, Pan T (2018) A plug-and-play, drug-on-pillar platform for combination drug screening implemented by microfluidic adaptive printing. Anal Chem 90(23):13969–13977. https://doi.org/10.1021/acs.analchem.8b03456
31. Lee W, Kim D, Rivnay J, Matsuhisa N, Lonjaret T, Yokota T, Yawo H, Sekino M, Malliaras GG, Someya T (2016) Integration of organic electrochemical and field-effect transistors for ultraflexible, high temporal resolution electrophysiology arrays. Adv Mater 28(44):9722–9728. https://doi.org/10.1002/adma.201602237
32. Song Y, Xu T, Xiu J, Zhang X (2020) Mini-pillar microarray for individually electrochemical sensing in microdroplets. Biosens Bioelectron 149:111845. https://doi.org/10.1016/j.bios.2019.111845
33. Teng IT, Li X, Yadikar HA, Yang Z, Li L, Lyu Y, Pan X, Wang KK, Tan W (2018) Identification and characterization of DNA aptamers specific for phosphorylation epitopes of tau protein. J Am Chem Soc 140(43):14314–14323. https://doi.org/10.1021/jacs.8b08645
34. Supraja P, Tripathy S, Vanjari SRK, Singh R, Singh V, Singh SG (2021) Label-free detection of β-amyloid (1-42) in plasma using electrospun SnO2 nanofiber based electro-analytical sensor. Sensors and Actuators B: Chemical 346. https://doi.org/10.1016/j.snb.2021.130522
35. Zubiate P, Urrutia A, Zamarreño CR, Egea-Urra J, Fernández-Irigoyen J, Giannetti A, Baldini F, Díaz S, Matias IR, Arregui FJ, Santamaría E, Chiavaioli F, Del Villar I (2019) Fiber-based early diagnosis of venous thromboembolic disease by label-free D-dimer detection. Biosensors and Bioelectronics: X 2:100026. https://doi.org/10.1016/j.biosx.2019.100026
36. Esposito F, Sansone L, Srivastava A, Baldini F, Campopiano S, Chiavaioli F, Giordano M, Giannetti A, Iadicicco A (2021) Long period grating in double cladding fiber coated with graphene oxide as high-performance optical platform for biosensing. Biosens Bioelectron 172:112747. https://doi.org/10.1016/j.bios.2020.112747
37. Chan HN, Xu D, Ho SL, Wong MS, Li HW (2017) Ultra-sensitive detection of protein biomarkers for diagnosis of Alzheimer's disease. Chem Sci 8(5):4012–4018. https://doi.org/10.1039/c6sc05615f
38. Kim K, Lee CH, Park CB (2020) Chemical sensing platforms for detecting trace-level Alzheimer's core biomarkers. Chem Soc Rev 49(15):5446–5472. https://doi.org/10.1039/d0cs00107d
39. Zhang X, Liu S, Song X, Wang H, Wang J, Wang Y, Huang J, Yu J (2019) Robust and universal SERS sensing platform for multiplexed detection of Alzheimer's disease core biomarkers using PAapt-AuNPs conjugates. ACS Sens 4(8):2140–2149. https://doi.org/10.1021/acssensors.9b00974
40. Kim H, Lee JU, Song S, Kim S, Sim SJ (2018) A shape-code nanoplasmonic biosensor for multiplex detection of Alzheimer's disease biomarkers. Biosens Bioelectron 101:96–102. https://doi.org/10.1016/j.bios.2017.10.018
41. Kim HJ, Ahn H, Kim H, Park D, Lee JS, Lee BC, Kim J, Yoon DS, Hwang KS (2022) Nanoparticle-based multiplex biosensor utilising dual dielectrophoretic forces for clinical diagnosis of Alzheimer's disease. Sens Actuators, B Chem 355:131288. https://doi.org/10.1016/j.snb.2021.131288
42. Kwon SS, Kim D, Yun M, Son JG, Lee SH (2021) The role of graphene patterning in field-effect transistor sensors to detect the tau protein for Alzheimer's disease: simplifying the immobilization process and improving the performance of graphene-based immunosensors. Biosens Bioelectron 192:113519. https://doi.org/10.1016/j.bios.2021.113519
43. Wang YR, Chuang HC, Tripathi A, Wang YL, Ko ML, Chuang CC, Chen JC (2021) High-sensitivity and trace-amount specimen electrochemical sensors for exploring the levels of beta-amyloid in human blood and tears. Anal Chem 93(22):8099–8106. https://doi.org/10.1021/acs.analchem.0c04980